EXPERIMENTAL EVALUATION OF PYROMETTALURGICAL PROCESSES FOR LEAD REMOVAL FROM BRASS

*S. Hilgendorf
Institute of Process Metallurgy and Metal Recycling (IME), RWTH Aachen / Fraunhofer Project Group Materials Recycling and Resource Strategies
Aachen, Germany
*(*Corresponding author: shilgendorf@ime-aachen.de)*

G. Homm, C. Gellermann and R. Stauber
Fraunhofer Project Group Materials Recycling and Resource Strategies
Alzenau, Germany

B. Friedrich
Institute of Process Metallurgy and Metal Recycling (IME), RWTH Aachen
Aachen, Germany

ABSTRACT

Due to recent regulations limiting tolerated lead concentrations in copper alloys, new recycling strategies have to be considered. This study investigates the suitability of technical approaches in order to recycle leaded copper alloys exemplified by CuZn39Pb2 and produce an alloy in compliance with future lead regulations in the European Union. Three pyrometallurgical methods are considered to achieve this goal, namely vacuum distillation, intermetallic precipitation and fractional crystallisation. The impact of essential process parameters i.e. pressure, temperature, time, atmosphere and quantity of additives are identified using thermochemical and kinetic modelling. An experimental implementation reveals a general suitability of all three refining processes. However, the individual efficiency of the different methods strongly differs. Thus, a detailed assessment is carried out in order to provide an evaluation on the efficiencies of these methods from a technological, economical and environmental point of view. Taking a possible industrial realisation into account, the authors recommend the approach of vacuum distillation, although the energy demanded is comparatively high due to the enthalpy of evaporation for zinc, or rather, lead. However, required lead concentrations can be reached quickly without introducing an external element to the material. The prediction of selectivity and evaporation speed, which are immanent variables for a successful implementation, can be validated experimentally.

KEYWORDS

Brass recycling, Fractional crystallisation, Intermetallic precipitation, Lead removal, Vacuum distillation

INTRODUCTION

In 2016 approximately 1 million tonnes of leaded copper alloy semi-finished goods with an average lead content of 2.1 Ma% have been produced in the European Union (EU). The global production in the same period exceeded 5.5 million tonnes, while the lead concentration has stayed constant at around 2.4 Ma% for the last 50 years. Up to 80 % of the current production volume is covered with end-of-life scraps, which are used for direct re-melting, depending on the alloy composition. Lead has been a popular alloying element in copper alloys in general, and in particular in brass due to its positive impact on various mechanical,

physical and chemical properties, especially machinability. Health and environmental concerns were drivers for many governments to implement limitations on lead. In order to further utilise the resource potential of leaded copper scrap, it is inevitable to develop methods to efficiently eliminate lead from circulation as far as possible. (Glöser, Soulier, & Tercero Espinoza, 2013; Soulier, Glöser-Chahoud, Goldmann & Tercero Espinoza, 2018)

CURRENT LEGAL SITUTATION AND DILUTION TROUBLE

Several regulations of the EU limit tolerated lead contents for, inter alia, toys, jewelry and watches, end-of-life-vehicles, waste electrical and electronic equipment and consumer products in general. For copper and copper alloys various exceptions are granted. Drinking water applications are not limited regarding its lead content, if the lead concentration in the water is below 10 µg/l. However, the so called 4MS initiative by the four member states Germany, France, the Netherlands and the United Kingdom has developed a 'Common Approach' in order to evaluate the suitability for drinking water materials in four categories and manifested the results on a 'Common Composition List'. In 2018 the highest tolerated lead concentration for product group B (e.g. fittings) is 2.2 Ma%, while pipes in building systems (product group A) have to be built with lead-free Cu-DHP. Table 1 gives an overview of existing regulations on several product groups regarding tolerated lead levels in copper or rather copper alloys in the EU. (European Union, 1998; European Union, 2000; European Union, 2003; European Union, 2008; European Union, 2009; 4MS, 2011; European Union, 2011; European Union, 2012; European Union, 2015; 4MS, 2016; European Union, 2016; European Union, 2017; 4MS, 2018)

Table 1. Lead regulations in the European Union

Product Group	Lead Limit	Latest Update
End-of-life vehicles	4.0 Ma%	2007
Waste Electrical and Electronic Equipment	4.0 Ma%	2011
Drinking Water Applications (Group B)	2.2 Ma%	2018
General Consumer Goods	0.5 Ma%	2016
Jewelry and Watches	500 ppm	2012
Toys	23 ppm	2018

A comprehensive study of global lead regulations for drinking water materials and their impact on the brass value chain has been published by Estelle (2016).

In order to implement the political guidelines while maintaining the end-of-life scrap input for copper alloy production, the re-melting industry has started to dilute the input material due to the lack of technical refining processes. Soulier, Glöser-Chahoud, Goldmann and Tercero Espinoza., however, showed that even until 2050 the average lead concentration in leaded copper alloys cannot be decreased below 0.6 Ma% with a diluting approach because end-of-life-scraps will show significant lead concentrations in the future (Soulier et al., 2018). If a short-term reduction of lead levels is supposed to be realised, alternative refining processes have to be considered. This paper presents three pyrometallurgical approaches in order to remove lead from the recycling loop of brass (CuZn39Pb2).

VACUUM DISTILLATION

The difference in vapour pressure of the elements as a function of temperature enables the procedure of vacuum distillation. As zinc has the highest vapour pressure in brass, this works aims at producing a pure zinc fraction in a first step and evaporating remaining zinc and lead completely in a second stage.

Thermodynamics

In real solutions the vapour pressure of the elements is influenced by its activity which again is strongly depended on the composition of the system according to equation 1 (Richardson, 1974).

$$p_i = a_i * p_i^0 = \gamma_i * x_i * p_i^0 \quad (1)$$

Using the thermochemical modelling software FactSage™ 7.2 allows the calculation of both, the vapour pressure of the pure substances and the activity coefficients for each element in the solution, i.e. copper, zinc and lead, for various compositions. All datasets are based on unmodified FactSage™ databases, i.e alloy related data is based on FSCopp database and FactPS database provides the data for the pure elements.

Based on these calculations the separation coefficient or rather the selectivity for the evaporation of the metals can be determined. For the first step of distillation the separation coefficient of zinc to lead gives the theoretical purity that can be achieved by the evaporation of zinc.

$$\beta_{Zn/Pb} = \frac{p_{Zn}}{p_{Pb}} \tag{2}$$

The vapour pressure ratio of zinc to lead as a function of the zinc concentration in brass with 58.0 Ma% copper and 2.0 Ma% lead for temperatures between 900 and 1100 °C is presented in Figure 1. From a thermodynamic perspective the temperature does not affect the selectivity of the process. With decreasing zinc contents the separation coefficient decreases as well due to the declining vapour pressure of zinc according to equation 1. With a distillate quality (zinc to lead) of 100 the zinc concentration is not to be set below 11.7 Ma%. However, this represents nearly 80 % of the initial zinc in the alloy, which can be distilled within the first step of vacuum distillation.

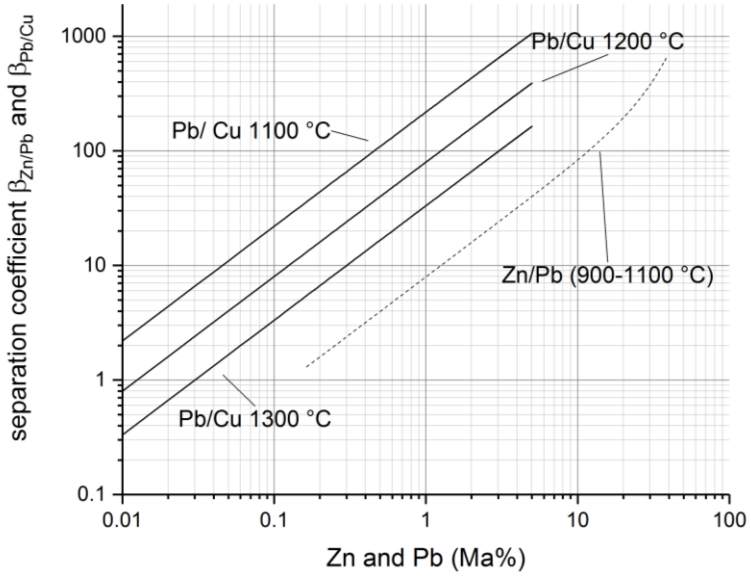

Figure 1. Impact of Zn or rather Pb concentrations on separation coefficients

To minimise copper losses in the second stage of distillation, the separation coefficient of lead to copper is calculated:

$$\beta_{Pb/Cu} = \frac{p_{Pb}}{p_{Cu}} \tag{3}$$

As indicated in Figure 1, the temperature has a crucial role regarding the selectivity of the separation of lead from copper. In order to achieve lead concentrations below 0.3 Ma%, the vapour pressure ratio drops from 66 at 1100 °C to 10 at 1300 °C. Therefore, the distillation preferably should be implemented at low temperatures from a thermodynamic point of view. The corresponding vapour pressure of 0.3 Ma% lead in copper at 1100 °C is $5*10^{-2}$ mbar. Hence, these are the optimum conditions in terms of minimal temperature at the maximum pressure to achieve the desired lead content.

Experimental implementation and results

The equipment used is a 4 kHz, 12 kg copper capacity, 40 kW or rather a 10 kHz, 6 kg copper capacity, 60 kW vacuum induction furnace. Continuous temperature measurement of the melt and the baffle or rather condenser is realised via type K thermocouples. All setup components are made of pure graphite if not stated otherwise. In the first step of distillation, ~ 6 kg of CuZn39Pb2 are heated to 950 °C in argon atmosphere at a pressure of 700 mbar. Slowly decreasing the pressure causes the evaporation of zinc which is then guided through a baffle to a condensing unit. The temperature is raised to 1100 °C at a constant atmospheric pressure of 200 mbar before decreasing the pressure isothermally to a value between 1 and 100 mbar. Final conditions are applied for 0 to 30 min to investigate the kinetics of the evaporation. For the second stage of distillation 2.5 kg of a synthetically produced CuPb3 alloy are heated to a temperature between 1100 and 1300 °C. After reducing the pressure to between 10^{-2} and 10^{0} mbar, kinetics are studied by examining the impact of holding times for up to 2 h. Evaporated lead is collected in a water cooled copper condensing unit.

The products analysed by Optical Emission Spectroscopy reveal a minimum lead contamination of the first stage condensate amounting to 0.5 Ma%, while the remaining zinc concentration in the corresponding ingot is 17 Ma%. The experimental selectivity validates its theoretical independence from applied temperatures. However, the achieved selectivity is higher than thermodynamic calculations predict. The results above thus suggests that the evaporation of lead is inhibited kinetically. In the second step of distillation lead contents of 500 ppm and lower can be achieved by applying pressures below 10^{-1} mbar at temperatures above 1100 °C. Raising copper losses at higher temperatures or rather lower pressures can be validated experimentally as well. Lead concentrations in the copper melt stagnate after 60 min at constant conditions.

A brass alloy containing lead levels below 0.3 Ma% can hence be produced using a two stage distillation with zinc losses below 10 % and a copper yield of 95 %.

INTERMETALLIC PRECIPITATION

Adding calcium to leaded brass provides the opportunity to remove lead due to the high affinity between to the two elements. Yamada, Fujimoto, Suehiro, Sueyoshi and Rochman (2002) published first results of this approach in 2002. Consequent work has been published by Nakano, Higashiiriki and Rochman (2005) as well as Sueyoshi, Miyazaki, Okada, Ashie and Kousaka (2018) and Sueyoshi et al. (2018).

Thermodynamics

It has been shown by the authors that temperature, amount of calcium and oxygen presence have a significant impact on the efficiency of lead removal (Hilgendorf, Binz, Welter & Friedrich, 2016). Depending on the amount of calcium added different calcium-lead-intermetallics are formed. According to the binary phase diagram of calcium-lead three stoichiometries of intermetallic phases (CaPb, Ca_5Pb_3 and Ca_2Pb) are stable above the liquidus temperature of CuZn39Pb2. A comparison of their densities with the one of brass shows that each of the three intermetallic compounds floats on liquid brass (Yang et al., 2010).

Figure 2 shows achievable lead contents in CuZn39Pb2 as a function of temperature for different calcium amounts. The calculations were carried out with FactSage™ 7.2. FSCopp provided the data for the liquid metal phase and FSLead was used to determine the formation of the intermetallic calcium-lead-phase. The temperature obviously is a crucial factor for the efficiency of the process due to its influence on the amount of dissoluble calcium in liquid brass. Hence, higher calcium amounts are necessary to achieve equivalent removal rates. As this is a thermodynamic consideration, the impact of process temperatures on the separation of formed intermetallic particles cannot be determined. Especially, the effect of lower viscosities of liquids with rising temperatures according to an Arrhenius equation is not considered.

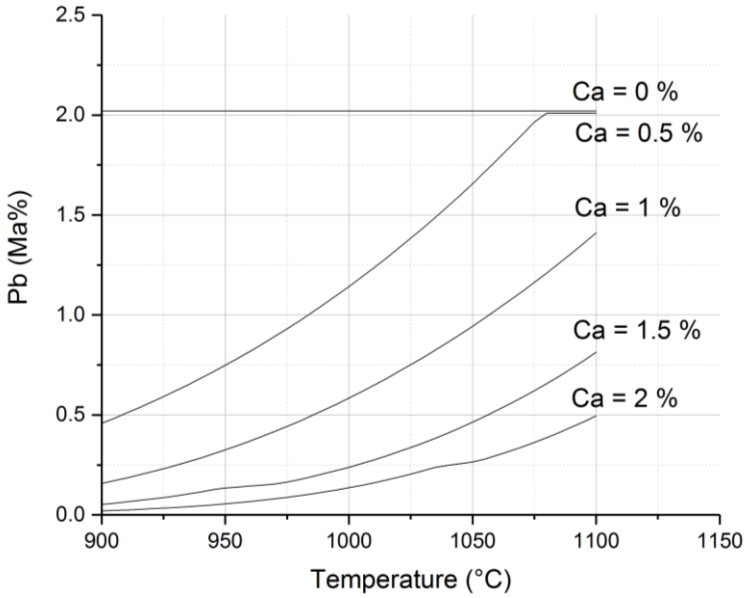

Figure 2. Effect of temperature and amount of calcium on achievable lead concentrations

Experimental implementation and results

The intermetallic precipitation of calcium-lead-phases is implemented in a 10 kHz vacuum induction furnace with 12 kg copper capacity and 40 kW. 2 kg of CuZn39Pb2 with varying amounts of calcium (0.7 – 2 Ma%) stemming from a commercially available copper-calcium master (CuCa10) alloy are charged in a clay-graphite crucible. Continuous temperature measurement is guaranteed via type K thermocouples in alumina protection tubes. The materials are heated in argon (1.1 bar) or air atmosphere to temperatures between 900 and 955 °C. Constant conditions are then applied for 3 to 35 min. The material solidifies in the crucible.

The results reveal a strong dependence of achieved lead removal rates on the process parameters. Air or rather the presence of oxygen in the atmosphere has a negative impact on the lead concentration in the product ingot. Sueyoshi et al. (2018) propose the oxidation of formed intermetallic phases and prove their existence in the brass matrix by SEM-EDS. Thereby, lead cannot be removed successfully, if oxygen is in contact with molten material. Implemented temperatures and calcium amounts confirm the results of the thermochemical modelling, namely increasing lead removal rates at low temperatures and high calcium amounts. For short dwell times the process efficiency increases. In a best case parameter combination the lead content is lowered to 0.3 Ma%. However, SEM-analysis shows a comprehensive presence of calcium-lead particles still remaining in the brass matrix. This suggests that not forming but separating the particles seems to be the problem. The remaining calcium-lead inclusions impair the mechanical properties such as tensile strength and elongation.

FRACTIONAL CRYSTALLISATION

Due to the well-documented small solubility of lead in copper or rather brass, lead has been a popular alloying element, which segregates on the grain boundaries and thereby improves several properties (Hutchinson & Rod, 2016). If the cooling process of leaded brass is realised slow enough, lead can be enriched in the liquid phase, while a lead-reduced brass matrix solidifies.

Thermodynamics

Brass forms a α+β-structure during solidification, if the zinc content in the binary mixture exceeds approximately 33 Ma%. The formation of the bcc β-phase is problematic to the extent that it shows a strong

solubility of lead and therefore a fractional crystallisation cannot occur, if the β-phase is formed during solidification (Materials Science International Team, 2007). Therefore, the zinc content of the brass used is decreased to 30 Ma% by diluting with pure copper in order to solely form fcc α-crystals.

The resulting part of the pseudo-binary system CuZn30-Pb provides the basis for further considerations. There are two significant differences compared to the CuZn39-Pb-system. The lead solubility in the solid phase is reduced to 1.7 Ma% (4 Ma% in CuZn39) at solidus temperature and the process area, which is given by the difference between liquidus and solidus temperature, is raised to 30 K (5 K in CuZn39).

The explanations made above are based on thermodynamic assumptions, especially regarding the concentration balance at all times. However, solidification processes are often characterised by differences in concentration between liquid and solid phases due to insufficient mass transport by diffusion in the solid phase. The concentration gradient can be calculated based on the work by Scheil and Gulliver (Marin-Alvarado, 2016). The approach neglects any mass transport in the solid phase and assumes that the concentration in the liquid phase is always balanced. This perspective depicts real cooling processes more exactly than cooling in thermodynamic equilibrium. Achievable concentrations with corresponding phase fraction amounts under ideal conditions are shown in Figure 3. The amount of lead in the liquid phase approaches 0 in thermodynamic equilibrium at solidus temperature (906 °C), while approximately 70 % can be enriched in the liquid phase according to Scheil-Gulliver-calculations. The corresponding lead concentration in the solid phase stays below 0.9 Ma% for Scheil-Gulliver-cooling. Although the lead concentration in the liquid phase reaches up to 6.5 Ma% at solidus temperature only small lead concentrations can be separated due to the small amount of the liquid phase fraction.

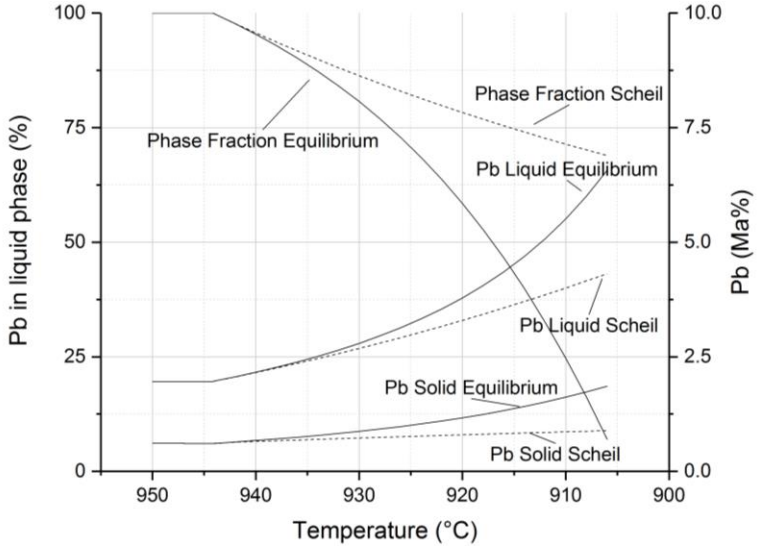

Figure 3. Phase fraction and lead concentrations during cooling assuming thermodynamic equilibrium and Scheil-Gulliver conditions

Experimental implementation and results

Experiments are carried out in a prototype furnace, which provides six individual heating zones. A temperature gradient can be realised vertically with each zone being controlled separately and an air cooled bottom plate for directed heat transfer. 6 kg of brass with zinc contents of 28-30 Ma% and 2 Ma% of lead are homogenised at 970 °C in a clay-graphite crucible before a cooling rate of 20-30 K/h is applied. The temperature is monitored on three positions (bottom, centre, top) via type K thermocouples in alumina protection tubes.

The ingots are analysed with respect to their chemical composition using Optical Emission Spectroscopy. Resulting lead concentrations for a cooling rate of 20 K/h and a temperature difference between the heating zones of 12 K are presented in Figure 4. The total time for solidification is four hours. It becomes visible that lead concentrations are lowered to below 1 Ma% for approximately 80 % of the ingot. Lead concentrations in the centre are higher compared to side concentrations in the upper part, where the overall content strongly increases.

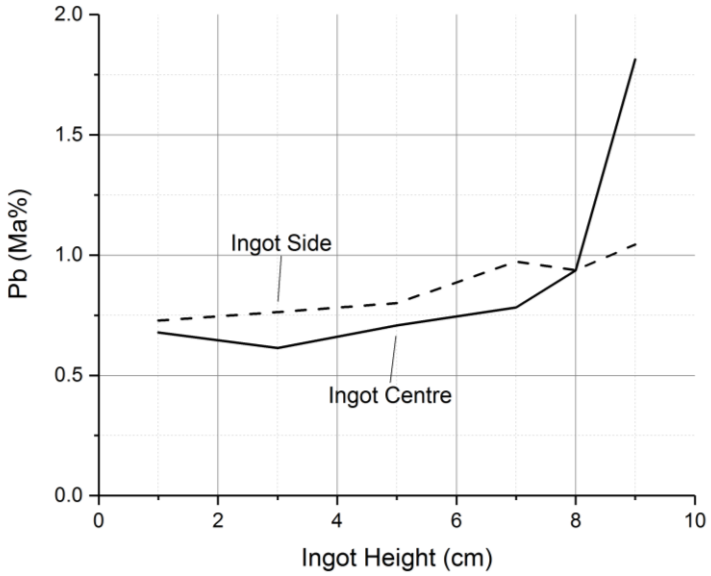

Figure 4. Lead concentrations in brass after fractional crystallisation as measured by Optical Emission Spectroscopy

DISCUSSION

Based on the results from thermochemical modelling and subsequent experimental implementation a comparison of the different strategies is carried out regarding the criteria as shown in Table 2.

Table 2. Comparison of lead-removal methods

	Vacuum Distillation	Intermetallic Precipitation	Fractional Crystallisation
Plant Complexity	Complex	Simple	Complex
Lead Removal Rate	> 90 %	> 80 %	> 50 %
Products	Cu, Zn, ZnPb	“Lead-free” Brass, CaPb containing Dross	“Lead-free” Brass, Lead-enriched Brass
Product Quality	High	Low	High
Material Yield	> 85 %	> 80 %	> 80 %
Throughput	High	High	Low
Energy Demand	High	Low	Low
Environmental Impact	Harmless	Critical	Harmless

Although, the effort and the energy demand of realising a vacuum process are comparatively high, vacuum distillation is the only process within this evaluation which provides required lead removal rates in an adequate period of time. Especially the concept of fractional crystallisation shows appreciably higher throughput times. The purity of obtained copper and zinc enables a direct usage as a lead-reduced brass in accordance with regulations of approximately 85 % of the initial material. Since all products are formed in the metallic state, there are no disposal concerns to be considered. The approach of intermetallic precipitation does not guarantee to form a high-quality product due to remaining calcium or rather calcium-lead intermetallic particles which impact the mechanical properties negatively. Since the by-product of vacuum

distillation (ZnPb) might be implemented in the de-silvering process (Parkes process) in extractive lead metallurgy, vacuum distillation fulfills the concept of zero-waste. As the intermetallic precipitation forms a dross containing calcium and lead without any known application, this fraction may have to be landfilled with a corresponding impact on the environment. The authors, therefore, focus on the investigation of vacuum distillation for further optimisation.

OPTIMISATION

As previously mentioned, the zinc concentration in the molten brass is the most crucial parameter on the quality or rather the lead content in the first stage of vacuum distillation because of its impact on the selectivity (see Figure 1). A kinetic model for the prediction of zinc evaporation is therefore evaluated based on Machlin's model of diffusion, the Hertz-Knudsen equation of evaporation and the gas phase mass transport based on Fick's law of diffusion or rather convection currents (Fick, 1855; Machlin, 1960; Kolasinski, 2012). The approach results in the following equation to calculate the mass flow of zinc as a function of temperature, pressure and power of the induction furnace:

$$\frac{\partial m}{\partial t} = \frac{x_0 \frac{M_{Zn}}{N_A} A_{melt}}{\frac{1}{K_{liquid}} + \frac{1}{K_{evaporation}} + \frac{1}{K_{gas}}} \tag{4}$$

with the individual particle flux densities

$$K_{liquid} = n_{liq} \cdot N_A \sqrt{\frac{8 \cdot D_{liquid} \cdot v_{liquid}}{\pi \cdot r_{cruc} \cdot h_{tot}^2 \cdot A_{melt}^2}} \tag{5}$$

$$K_{evaparation} = \frac{\alpha_{evaporation} \cdot p_{Zn}^0 \cdot \gamma_{Zn} \cdot N_A}{\sqrt{2 \cdot \pi \cdot M_{Zn} \cdot R \cdot T_{liquid}}} \tag{6}$$

$$K_{gas} = \frac{\beta_{gas} \cdot N_A \cdot p_{Zn}^0 \cdot \gamma_{Zn}}{R \cdot T_{gas}} \tag{7}$$

These kinetics neglect the mass transport in the bulk liquid metal phase and condensation, as well as heat transfer. Several authors, however, have published similar mathematics describing the kinetics of vacuum distillation. (Harris, 1984; Ozberk & Guthrie, 1986; Harris & Davenport, 1992; Blacha and Labaj, 2012; Safarian & Tangstad, 2012).

The calculated trend of the zinc concentration based on the kinetic model can be validated experimentally (see Figure 5) and thereby help to implement to realise small lead contents in the condensate of the first stage of vacuum distillation. According to the calculation, the mass transport in the gas phase limits the speed of the total distillation in the beginning before the mass transport in the liquid phase is predominant. The increasing number of atoms, which can be transported in the gas phase, is due to the decreasing atmospheric pressure. Although the evaporation mass transfer decreases because of its dependence on the vapour pressure, the evaporation does not become the predominant step.

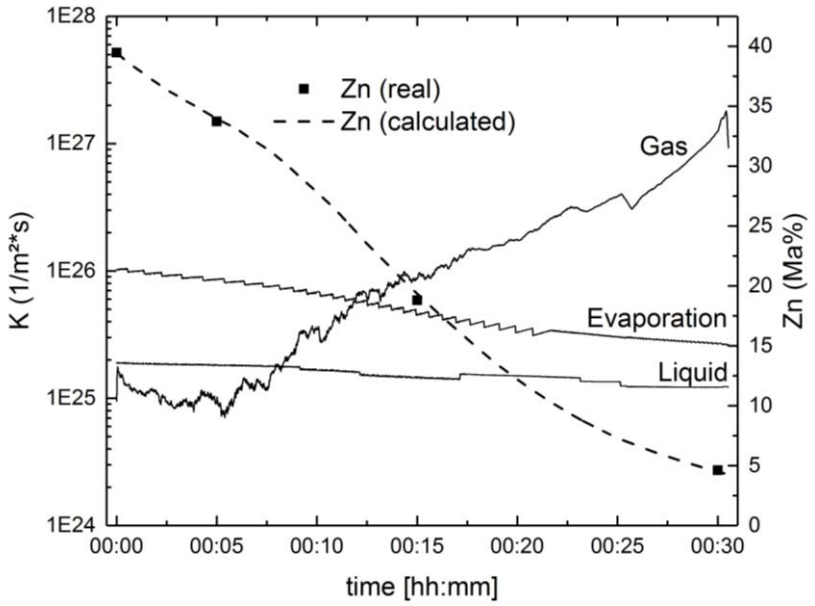

Figure 5. Calculated zinc concentration and mass transfer coefficients during distillation

CONCLUSIONS

Three technologies providing the opportunity to remove lead from molten brass were studied from a thermochemical point of view and investigated experimentally. Considering a list of criteria, a two-stage distillation process is the most balanced approach to produce high quality lead-reduced brass in a short time without generating critical by-products. Based on a kinetic model the evaporation speed of zinc during distillation can be determined in order to control the lead contamination of the condensate. The model also reveals the limiting mass transfer factors for distilling and thereby discloses a further optimisation of the process regarding both selectivity and throughput.

NOMENCLATURE

a_i	activity of element i	p_i^0	pure substance vapour pressure of element i
A_{melt}	melt surface area	R	universal gas constant
D_{liquid}	diffusion coefficient in the liquid phase	r_{cruc}	crucible radius
h_{tot}	total height of the melt	t	time
$K_{evaporation}$	total particle flux density of evaporation	T_{gas}	gas phase temperature
K_{gas}	total particle flux density in the gas phase	T_{liquid}	melt temperature
K_{liquid}	total particle flux density in the liquid phase	v_{liquid}	melt surface velocity
m	mass	x_0	initial mole fraction of Zn in brass
Ma%	percentage by mass	$\alpha_{evaporation}$	volatility coefficient
M_{Zn}	molar mass of Zn	β_{gas}	gas phase mass transfer coefficient
N_A	Avogadro constant	$\beta_{i/j}$	separation coefficient between elements i and j
n_{liq}	total amount of liquid substance	γ_{Zn}	activity coefficient of Zn
p_i	vapour pressure of element i		

REFERENCES

4MS Joint Management Committee (2011). Declaration of Intent between the competent authorities of France, Germany, the Netherlands und and the United Kingdom concerning the approval of products in contact with drinking water (drinking water quality).

4MS Joint Management Committee (2016). Acceptance of metallic materials used for products in contact with drinking water. Part A – Procedure for the acceptance. 2nd Revision.

4MS Joint Management Committee (2018). Acceptance of metallic materials used for products in contact with drinking water. Part B – 4MS Common Composition List. 9th Revision.

Blacha, L., & Labaj, J. (2012). Factors determining the rate of the process of metal bath components evaporation. *Metalurgija/Metallurgy*, *51*(4), 529-533.

Estelle, A. A. (2016). Drinking water lead regulations: impact on the brass value chain. *Materials Science and Technology*, *32*(17), 1763-1770. https://doi.org/10.1080/02670836.2016.1220906

European Union (2017). Council Directive (EU) 2017/738 of 27 March 2017 amending, for the purpose of adapting to technical progress, Annex II to Directive 2009/48/EC of the European Parliament and of the Council on the safety of toys, as regards lead.

European Union (2016). Commission Regulation (EU) 2016/1179 of 19 July 2016 amending, for the purposes of its adaptation to technical and scientific progress, Regulation (EC) No 1272/2008 of the European Parliament and of the Council on classification, labelling and packaging of substances and mixtures.

European Union (2015). Commission Regulation (EU) 2015/628 of 22 April 2015 amending Annex XVII to Regulation (EC) No 1907/2006 of the European Parliament and of the Council on the Registration, Evaluation, Authorisation and Restriction of Chemicals ('REACH') as regards lead and its compounds.

European Union (2012). Commission Regulation (EU) No 836/2012 of 18 September 2012 amending Annex XVII to Regulation (EC) No 1907/2006 of the European Parliament and of the Council on the Registration, Evaluation, Authorisation and Restriction of Chemicals (REACH) as regards lead.

European Union (2011). Directive 2011/65/EU of the European Parliament and of the Council of 8 June 2011 on the restriction of the use of certain hazardous substances in electrical and electronic equipment.

European Union (2009). Directive 2009/48/EC of the European Parliament and of the Council of 18 June 2009 on the safety of toys.

European Union (2008). Regulation (EC) No 1272/2008 of the European Parliament and of the Council of 16 December 2008 on classification, labelling and packaging of substances and mixtures, amending and repealing Directives 67/548/EEC and 1999/45/EC, and amending Regulation (EC) No 1907/2006.

European Union (2003). Directive 2002/95/EC of the European Parliament and of the Council of 27 January 2003 on the restriction of the use of certain hazardous substances in electrical and electronic equipment.

European Union (2000). Directive 2000/53/EC of the European Parliament and of the Council of 18 September 2000 on end-of-life vehicles.

European Union (1998). Council Directive 98/83/EC of 3 November 1998 on the quality of water intended for human consumption.

Fick, A. (1855). Concerns diffusion and concentration gradient. *Annalen der Physik*, *170*(59), 13.

Glöser, S., Soulier, M., & Tercero Espinoza, L. A. (2013). Dynamic analysis of global copper flows. Global stocks, postconsumer material flows, recycling indicators, and uncertainty evaluation. *Environmental science & technology*, *47*(12), 6564-6572. https://doi.org/10.1021/es400069b

Harris, R. (1984). Vacuum refining copper melts to remove bismuth, arsenic, and antimony. *Metallurgical Transactions B*, *15*(2), 251-257. https://doi.org/10.1007/BF02667328

Harris, R., & Davenport, W. G. (1992). Vacuum distillation of liquid metals: Part I. Theory and experimental study. *Journal of Electronic Materials*, *21*(1), 581-588. https://doi.org/10.1007/BF02669171

Hilgendorf, S., Binz, F., Welter, J. M., & Friedrich, B. (2016). Lead removal from brass scrap by fluorine-free compound separation. *Materials Science and Technology*, *32*(17), 1782-1788. https://doi.org/10.1080/02670836.2016.1223574

Hutchinson, B., & Rod, O. (2016). Brass alloys. *Materials Science and Technology*, *32*(17), 1743. https://doi.org/10.1080/02670836.2016.1240325

Kolasinski, K. W. (2012). Surface science: foundations of catalysis and nanoscience. John Wiley & Sons. https://doi.org/10.1002/9781119941798

Machlin, E. S. (1960). Kinetics of vacuum induction refining-theory. *Transactions of the American Institute of Mining and Metallurgical Engineers*, *218*(2), 314-326.

Marin-Alvarado, T. (2016). Modelling Scheil Cooling of a Metal Alloy–Thermodynamic and Multiphysics Solidification. *Proceedings of the 2016 COMSOL Conference*.

Materials Science International Team MSIT® info@ msiwp. com http://www. matport. com. (2007). Cu-Pb-Zn (Copper-Lead-Zinc) Non-Ferrous Metal Ternary Systems. Selected Copper Systems: Phase Diagrams, Crystallographic and Thermodynamic Data. *Non-Ferrous Metal Systems. Part 2: Selected Copper Systems*, 408-419.

Nakano, A., Higashiiriki, K., & Rochman, N. T. (2005). Removal of lead from brass scrap by compound-separation method. *Journal of the Japan institute of Metals*, *69*(2), 198-201.

Richardson, F. D. (1974). *Physical chemistry of melts in metallurgy* (Vol. 1). Academic press.

Ohno, R. (1991). Kinetics of removal of bismuth and lead from molten copper alloys in vacuum induction melting. *Metallurgical transactions B*, *22*(4), 447-465. https://doi.org/10.1007/BF02654283

Ozberk, E., & Guthrie, R. I. L. (1986). A kinetic model for the vacuum refining of inductively stirred copper melts. *Metallurgical Transactions B*, *17*(1), 87-103. https://doi.org/10.1007/BF02670822

Safarian, J., & Tangstad, M. (2012). Vacuum refining of molten silicon. *Metallurgical and Materials Transactions B*, *43*(6), 1427-1445. https://doi.org/10.1007/s11663-012-9728-1

Soulier, M., Glöser-Chahoud, S., Goldmann, D., & Tercero Espinoza, L. A. (2018). Dynamic analysis of European copper flows. *Resources, Conservation and Recycling*, *129*, 143-152. https://doi.org/10.1016/j.resconrec.2017.10.013

Sueyoshi, H., Yamada, K., Miyazaki, M., Okada, T., Ashie, N. and Kousaka, Y. (2018) Mechanism of Pb Removal from Brass Scrap by Compound Separation Using Ca and NaF. *International Journal of Nonferrous Metallurgy*, *7*, 1-7. https://doi.org/10.4236/ijnm.2018.71001

Sueyoshi, H., Miyazaki, M., Okada, T., Ashie, N. and Kousaka, Y. (2018) The Kinetics of Pb Removal from Brass Scrap Using Compound Separation. *International Journal of Non-ferrous Metallurgy*, *7*, 39-55. https://doi.org/10.4236/ijnm.2018.74004

Yamada, K., Fujimoto, R., Suehiro, S. I., Sueyoshi, H., & Rochman, N. T. (2002). Removal of lead from scrap brass. *Journal of advanced science*, *13*(3), 273-276. https://doi.org/10.2978/jsas.13.273

Yang, Z., Shi, D., Wen, B., Melnik, R., Yao, S., & Li, T. (2010). First-principle studies of Ca–X (X= Si, Ge, Sn, Pb) intermetallic compounds. *Journal of Solid State Chemistry*, *183*(1), 136-143. https://doi.org/10.1016/j.jssc.2009.11.007